

A NYSTRÖM METHOD FOR WEAKLY SINGULAR INTEGRAL OPERATORS ON SURFACES

JAMES BREMER^{*,‡} AND ZYDRUNAS GIMBUTAS[†]

ABSTRACT. We describe a modified Nyström method for the discretization of the weakly singular boundary integral operators which arise from the formulation of linear elliptic boundary value problems as integral equations. Standard Nyström and collocation schemes proceed by representing functions via their values at a collection of quadrature nodes. Our method uses appropriately scaled function values in lieu of such representations. This results in a scheme which is mathematically equivalent to Galerkin discretization in that the resulting matrices are related to those obtained by Galerkin methods via conjugation with well-conditioned matrices, but which avoids the evaluation of double integrals. Moreover, we incorporate a new mechanism for approximating the singular integrals which arise from the discretization of weakly singular integral operators which is considerably more efficient than standard methods. We illustrate the performance of our method with numerical experiments.

In this article, we describe a mechanism for the discretization of a class of integral operators which arise from the formulation of elliptic boundary value problems as integral equations. More specifically, we treat boundary integral operators of the form

$$Tf(q) = \iint_{\Sigma} K(q, p)f(p)ds(p) \tag{1}$$

with K a weakly singular kernel associated with an elliptic partial differential operator and Σ a piecewise smooth surface. Galerkin methods are typically used to discretize operators of this sort [2, 10]. A common variant calls for choosing an appropriate orthonormal set $\{u_1, u_2, \dots, u_n\}$ in $L^2(\Sigma)$ and forming the $n \times n$ matrix A with elements

$$A_{ij} = \langle u_i, Tu_j \rangle, \tag{2}$$

where $\langle \cdot, \cdot \rangle$ denotes the $L^2(\Sigma)$ inner product. The matrix A constructed in this fashion enjoys a straightforward relationship with the operator T . If we let S be the subspace spanned by u_1, \dots, u_n , denote by P the orthogonal projection of $L^2(\Sigma)$ onto S , and define $\Phi : S \rightarrow \mathbb{C}^n$ by

$$\Phi \left(\sum_{j=1}^n \alpha_j u_j \right) = \begin{pmatrix} \alpha_1 \\ \alpha_2 \\ \vdots \\ \alpha_n \end{pmatrix}$$

then the diagram

$$\begin{array}{ccc} S \subset L^2(\Sigma) & \xrightarrow{PTP} & S \subset L^2(\Sigma) \\ \downarrow \Phi & & \downarrow \Phi \\ \mathbb{C}^n & \xrightarrow{A} & \mathbb{C}^n \end{array} \tag{3}$$

commutes. Since Φ is an isomorphism of $S \subset L^2(\Sigma)$ with \mathbb{C}^n , it follows that the matrix A inherits many of the properties of the operator T . For instance, the condition number of the matrix A approximates that of the operator $T : L^2(\Sigma) \rightarrow L^2(\Sigma)$. Note that the functions u_j are typically constructed through geometric subdivision of Σ and each one is usually supported on a proper subset of Σ rather than on the entire surface.

^{*}Department of Mathematics, University of California, Davis, Davis CA 95616 USA.

[†]Courant Institute of Mathematical Sciences, New York University, New York, NY 10012 USA.

[‡]Corresponding author. *E-mail address*: bremer@math.ucdavis.edu.

The Galerkin method described above has the advantage that the discretizations which result from applying it the weakly singular integral operators are generally well-conditioned, even when those operators are given on piecewise smooth surfaces. This is in contrast to standard Nyström and collocation methods, which usually do not produce well-conditioned linear systems when applied to integral operators given on Lipschitz domains; see, for instance, [4] for examples of the ill-conditioning resulting from the application of standard Nyström and collocation methods to integral operators given on planar curves with corners.

The Galerkin method’s advantages come at a price, however: computation of the inner products (2) requires the evaluation of double integrals of the form

$$\iint_{\Sigma} \left(\iint_{\Sigma} K(q, p) u_j(p) ds(p) \right) u_i(q) ds(q). \quad (4)$$

Numerical approximation of four-dimensional integrals of this type, which is inherently expensive, is further complicated when the kernel K is weakly singular. In particular, the inner integral in (4) presents challenges when K is a weakly singular kernel and q is either in the support of the function u_j or close to the support of the function u_j . We will refer to the first case as the “singular” case and the second as the “nearly singular” case. A common approach to the evaluation of these integrals calls for first changing the variables of integration so as to eliminate or ameliorate the singularity in the kernel K and then applying an adaptive integration procedure [15, 16, 11]. In another popular approach, graded meshes and hp methods are employed to address kernel singularities or near singularities [13, 6]. Both approaches, however, are prohibitively expensive in certain circumstances. For instance, most adaptive schemes perform poorly when the aspect ratio of the support of the function u_j is large or when the point q is close to the boundary of the support of u_j .

In this article, we introduce a modified Nyström scheme for the discretization of operators of the form (1) which is a generalization of the schemes of [3, 4] for integral operators given on planar curves with singular points. It captures the action of an integral operator on spaces of square integrable functions rather than its pointwise behavior but without the need to evaluate double integrals. An orthonormal set of functions $\{u_1, u_2, \dots, u_n\}$ is introduced and plays much the same role as it does in the Galerkin method. In this article, the u_j are generated from polynomials of a certain fixed order on the standard simplex. This yields an approximation error which depends algebraically on the quantity

$$\max_j |\text{supp}(u_j)|,$$

where $\text{supp}(u_j)$ refers to the support of the function u_j and $|E|$ is used to indicate the diameter of the set E . Exponential convergence can be obtained by representing solutions in terms of global basis functions rather than locally supported basis functions, by introducing partitions of unity, or by switching to hp -type representations of solutions (that is, by allowing the order of the polynomials used to represent solutions to vary). In this article our focus is on reducing the constants in the running time of boundary element schemes, which are principally dependent on the costs incurred while evaluating the integrals which arise in the discretization of integral operators. As a result, we settle for algebraic convergence and leave the development of exponentially convergent variants of our scheme for future work.

We also introduce a novel mechanism for the evaluation of singular integrals of the form

$$\iint_{\Sigma} K(q, p) u_j(p) ds(p), \quad (5)$$

where K is a weakly singular kernel associated with an elliptic partial differential equation and q is a point in the support of u_j . It proceeds by first applying a suitable transformation in order to simplify the integrand and then using a precomputed table of quadrature rules to evaluate the resulting integral efficiently. The performance of the precomputed quadrature rules is much less dependent on the geometry of $\text{supp}(u_j)$ than adaptive methods, which means that the number of nodes required to evaluate singular integrals is substantially reduced when the support of the function u_j is irregular. It does, however, have two significant drawbacks vis-à-vis adaptive integration methods. First, a restricted class of weakly singular kernels must be chosen at the time of the precomputations. The class of kernels can be expanded by recomputing new quadrature rules, but some class must be fixed *a priori*. For the experiments of this paper, we used a collection of quadrature rules which apply to operators arising from the Neumann and Dirichlet problems for Laplace’s equation and the Helmholtz equation as well the operators associated with the magnetic field integral equation. Second, the approximation of the integral (5) depends algebraically on the diameters of $\text{supp}(u_j)$. This is quite different

from most adaptive schemes which yield a specified accuracy independent of such considerations. The rate of convergence is fixed at the time of the quadrature precomputation and can be set arbitrarily high (of course, higher orders lead to larger quadrature rules). However, if the order of the precomputed quadrature rules is chosen to be sufficiently high, then the rate of convergence of the Nyström scheme *in toto* is unaffected. That is, under typical conditions, when discretizations resulting from the scheme of this article are used to solve integral equations, the resulting error is dominated by the error arising from the approximation of solutions of the integral equation as polynomials and not by the errors incurred approximating the integrals (5).

This article is structured as follows. In Section 1, we introduce several pieces of notation and review certain well-known mathematical constructs which will be used throughout this article. Section 2 describes the Nyström scheme proper, although a discussion of the evaluation of singular integrals of the form (5) is deferred to Section 3. Section 4 describes a collection of numerical experiments performed to assess the effectiveness of our approach and the article concludes with a discussion in Section 5 of future avenues of investigation related to approach described in this paper.

1. PRELIMINARIES

1.1. Koornwinder polynomials. The Jacobi polynomial $\phi_k^{(\alpha,\beta)}$ is the analytic solution of the second order linear homogeneous differential equation

$$(1-x^2)y''(x) + (\beta - \alpha - (\alpha + \beta + 2)x)y'(x) + k(k + \alpha + \beta + 1)y(x) = 0, \quad -1 < x < 1.$$

See [1] or [18] for a discussion of the properties of Jacobi polynomials. In [12], it was observed that the $(N+1)(N+2)/2$ functions

$$\psi_{k,n}(x, y) = \phi_{n-k}^{(2k+1,0)}(2x-1) \phi_k^{(0,0)}\left(\frac{2y}{1-x} - 1\right) (1-x)^k, \quad k = 0, \dots, n, \quad n = 0 \dots N,$$

form an orthogonal basis for the space \mathcal{P}_N of polynomials of degree at most N on the standard simplex

$$\Delta^1 = \{(x, y) \in \mathbb{R}^2 : 0 \leq x \leq 1, 0 \leq y \leq 1-x\}.$$

It will sometimes be convenient to instead consider the normalized functions $\tilde{\psi}_{k,n}$ defined by

$$\tilde{\psi}_{k,n} = \frac{\psi_{k,n}}{\|\psi_{k,n}\|_2}.$$

Here, $\|\cdot\|_2$ is the $L^2(\Delta^1)$ norm. In what follows, we shall refer to the $\psi_{k,n}$ as the Koornwinder polynomials and the $\tilde{\psi}_{k,n}$ as the normalized Koornwinder polynomials.

1.2. Quadrature and interpolation of polynomials on triangles. We say that a quadrature formula of the form

$$\iint_{\Delta^1} f(x, y) dx dy \approx \sum_{j=1}^n f(x_j, y_j) w_j, \quad (6)$$

where Δ^1 once again denotes the standard simplex, is exact for a collection of functions f_1, \dots, f_n defined on Δ^1 if

$$\iint_{\Delta^1} f_i(x, y) dx dy = \sum_{j=1}^n f_i(x_j, y_j) w_j, \quad i = 1, \dots, n.$$

The points (x_j, y_j) are referred to as quadrature nodes while the w_j are called quadrature weights. Moreover, we say that the length of a quadrature rule of the form (6) is equal to the number of terms n appearing on the right-hand side.

A quadrature rule of length $\dim \mathcal{P}_N = (N+1)(N+2)/2$ whose weights are positive and which is exact for the polynomials in \mathcal{P}_{2N} is called a Gaussian quadrature rule. Such rules are true generalizations of one-dimensional Legendre quadrature rules which allow spaces of polynomials to be isomorphically embedded via scaled function values. That is, if

$$(x_1, y_1), \dots, (x_l, y_l), \quad w_1, \dots, w_l$$

are the nodes and weights of a Gaussian quadrature of length $l = (N + 1)(N + 2)/2$, then the mapping $\Phi : \mathcal{P}_N \rightarrow \mathbb{R}^l$ defined by

$$\Phi(f) = \begin{pmatrix} f(x_1, y_1)\sqrt{w_1} \\ f(x_2, y_2)\sqrt{w_2} \\ \vdots \\ f(x_l, y_l)\sqrt{w_l} \end{pmatrix} \quad (7)$$

is an isomorphism. Moreover, the $l \times l$ matrix

$$A = \begin{pmatrix} \tilde{\psi}_{0,0}(x_1, y_1)\sqrt{w_1} & \tilde{\psi}_{0,0}(x_2, y_2)\sqrt{w_2} & \cdots & \tilde{\psi}_{0,0}(x_l, y_l)\sqrt{w_l} \\ \tilde{\psi}_{0,1}(x_1, y_1)\sqrt{w_1} & \tilde{\psi}_{0,1}(x_2, y_2)\sqrt{w_2} & \cdots & \tilde{\psi}_{0,1}(x_l, y_l)\sqrt{w_l} \\ \tilde{\psi}_{1,1}(x_1, y_1)\sqrt{w_1} & \tilde{\psi}_{1,1}(x_2, y_2)\sqrt{w_2} & \cdots & \tilde{\psi}_{1,1}(x_l, y_l)\sqrt{w_l} \\ \vdots & \vdots & \ddots & \vdots \\ \tilde{\psi}_{n,n}(x_1, y_1)\sqrt{w_1} & \tilde{\psi}_{n,n}(x_2, y_2)\sqrt{w_2} & \cdots & \tilde{\psi}_{n,n}(x_l, y_l)\sqrt{w_l} \end{pmatrix}, \quad (8)$$

which maps the scaled values

$$\begin{pmatrix} f(x_1, y_1)\sqrt{w_1} \\ f(x_2, y_2)\sqrt{w_2} \\ \vdots \\ f(x_l, y_l)\sqrt{w_l} \end{pmatrix} \quad (9)$$

of a function f in \mathcal{P}_N to the coefficients $\{\alpha_{i,j}\}$ in the expansion

$$f(x, y) = \sum_{j=0}^N \sum_{i=0}^j \alpha_{i,j} \tilde{\psi}_{i,j}(x, y)$$

of f as a sum of normalized Koornwinder polynomials will be orthogonal. If

$$(u_1, v_1), \dots, (u_k, v_k), r_k, \dots, r_k \quad (10)$$

are the nodes and weights of a second quadrature exact for the polynomials in \mathcal{P}_{2N} , then the matrix

$$B = \begin{pmatrix} \tilde{\psi}_{0,0}(u_1, v_1)\sqrt{r_1} & \tilde{\psi}_{0,1}(u_1, v_1)\sqrt{r_1} & \tilde{\psi}_{1,1}(u_1, v_1)\sqrt{r_1} & \cdots & \tilde{\psi}_{n,n}(u_1, v_1)\sqrt{r_1} \\ \tilde{\psi}_{0,0}(u_2, v_2)\sqrt{r_2} & \tilde{\psi}_{0,1}(u_2, v_2)\sqrt{r_2} & \tilde{\psi}_{1,1}(u_2, v_2)\sqrt{r_2} & \cdots & \tilde{\psi}_{n,n}(u_2, v_2)\sqrt{r_2} \\ \vdots & \vdots & \ddots & \vdots & \vdots \\ \tilde{\psi}_{0,0}(u_k, v_k)\sqrt{r_k} & \tilde{\psi}_{0,1}(u_k, v_k)\sqrt{r_k} & \tilde{\psi}_{1,1}(u_k, v_k)\sqrt{r_k} & \cdots & \tilde{\psi}_{n,n}(u_k, v_k)\sqrt{r_k} \end{pmatrix} \quad (11)$$

has orthonormal columns. It follows that the interpolation matrix BA , which takes scaled values of a function f in \mathcal{P}_N at the nodes of the Gaussian quadrature to its scaled values at the nodes of the quadrature (10), is well-conditioned. In fact, all of the singular values of BA are either be 1 or 0.

Lamentably, the construction of Gaussian quadrature rules for polynomials of reasonable orders on triangles appears to be a very challenging problem. In [19], a procedure for the construction of quadrature formulae for polynomials on convex planar regions is introduced. These quadratures are not Gaussian in the sense defined above, but they do have the property that the quadrature formula of length $(N + 1)(N + 2)/2$ integrates polynomials of degree less than or equal to M , with $M > N$. While it is still invertible, the mapping (7) associated with one of these quadrature rules is no longer an isomorphism of \mathcal{P}_N with $\mathbb{R}^{(N+1)(N+2)/2}$ in that it distorts inner products. Moreover, the matrix (8) is no longer orthonormal. Some care was taken by the authors of [19], however, to minimize the distortion of inner products introduced into the mapping Φ and the condition numbers of the interpolation matrices associated with these quadrature rules. See [19] for a further discussion of the issue. These quadrature rules play an important role in the discretization procedure described in Section 2 and we shall refer to quadrature rule of length $(N + 1)(N + 2)/2 = \dim \mathcal{P}_N$ on the simplex Δ^1 constructed using the procedure of [19] as the Vioreanu-Rokhlin rule of order N .

1.3. Generalized quadrature. This section concerns the numerical construction of quadrature rules of the form

$$\int_0^1 f(x)dx \approx \sum_{j=1}^M f(x_j)w_j \tag{12}$$

which integrate a specified subspace S of functions in $L^2([0,1])$. The subspace S will be described by a spanning set f_1, \dots, f_n of functions which we will assume are pointwise defined in $(0,1)$. The condition that the quadrature rule (12) integrates functions in S is equivalent to requiring that the system of equations

$$\sum_{j=1}^N f_i(x_j)w_j = \int_0^1 f_i(x)dx, \quad i = 1, \dots, n, \tag{13}$$

be satisfied. Of course, since we concerned with a numerical procedure, we will have to content ourselves with quadrature rules for which (13) holds to a high degree of accuracy. We are interested in constructing quadrature rules of minimum possible length and we now describe a technique for obtaining quadrature formulae with approximately $\frac{1}{2} \dim S$ nodes. The discussion here is cursory; the article [5], which introduces the method, describes it in considerably more detail.

First suppose that $\{f_1, \dots, f_n\}$ is an orthonormal set of functions in $L^2([-1,1])$ spanning the subspace S and

$$x_1, \dots, x_m, w_1, \dots, w_m$$

are the nodes and weights of a quadrature which integrates products of the f_j , but with $m \gg n$. Then a quadrature rule of length n can be constructed by viewing (13) as a linear system with the weights w_j as unknowns. More specifically, one forms the linear system of equations

$$\begin{pmatrix} f_1(x_1)\sqrt{w_1} & f_1(x_2)\sqrt{w_2} & \cdots & f_1(x_m)\sqrt{w_m} \\ f_2(x_1)\sqrt{w_1} & f_2(x_2)\sqrt{w_2} & \cdots & f_2(x_m)\sqrt{w_m} \\ \vdots & & \ddots & \vdots \\ f_n(x_1)\sqrt{w_1} & f_n(x_2)\sqrt{w_2} & \cdots & f_n(x_m)\sqrt{w_m} \end{pmatrix} \begin{pmatrix} v_1 \\ v_2 \\ \vdots \\ v_m \end{pmatrix} = \begin{pmatrix} b_1 \\ b_2 \\ \vdots \\ b_n \end{pmatrix}, \tag{14}$$

where

$$b_i = \int_0^1 f_i(x)dx, \quad i = 1, \dots, n. \tag{15}$$

Because the rank of the matrix given the coefficients of this linear system is n , a rank-revealing QR factorization can be used to construct a solution

$$\begin{pmatrix} z_1 \\ z_2 \\ \vdots \\ z_m \end{pmatrix}$$

of (14) with no more than n nonzero entries. If we label those entries

$$z_{i_1}, z_{i_2}, \dots, z_{i_n}$$

then

$$\int_0^1 f(x)dx \approx \sum_{l=1}^n f(x_{i_l})z_{i_l}\sqrt{w_{i_l}}$$

is a quadrature rule of length n which integrates the f_j . Note that the matrix appearing in (14) has singular values which are either 1 or 0 owing to the assumption that the initial quadrature rule integrates products of the functions in the orthonormal set $\{f_1, \dots, f_n\}$. The stability of this approach is discussed in more detail in [5].

By viewing (13) as a nonlinear system of equations in the nodes x_j and in the weights w_j , we can further reduce the length of the quadrature rule obtained by solving the linear system (14). Let

$$y_1, \dots, y_l, v_1, \dots, v_l$$

denote a quadrature formula which integrates the f_j . In order to reduce the length of the formula by 1, we first delete one of the points in the quadrature rule and then use the remaining nodes and weights as an initial guess for the Gauss-Newton method, which is applied to the nonlinear system

$$F_i(x_1, \dots, x_{l-1}, w_1, \dots, w_{l-1}) = b_i, \quad i = 1, \dots, n,$$

where F_1, \dots, F_n are defined by

$$F_i(x_1, \dots, x_{l-1}, w_1, \dots, w_{l-1}) = \sum_{r=1}^{l-1} f_i(x_r) w_r$$

and the b_i are as in (15). If suitable accuracy is obtained, then the reduced quadrature rule is accepted. If not, then another point is chosen and the quadrature rule obtained by deleting it is used as an initial guess for the Gauss-Newton method. This procedure is repeated until either a point is successfully eliminated or no point can be eliminated without reducing accuracy.

By repeatedly applying this algorithm for eliminating one quadrature node, a rule with approximately $\frac{1}{2} \dim S$ nodes can generally be formed.

Now suppose that the f_1, \dots, f_n specified by the user do not form an orthonormal basis for S , but are instead a spanning set with $n > \dim S$. First, an oversampled quadrature $x_1, \dots, x_m, w_1, \dots, w_m$ which integrates products of the given functions f_1, \dots, f_n is constructed via adaptive integration. Then an orthonormal basis for the span of S is obtained by applying the pivoted Gram-Schmidt procedure to the columns of the matrix

$$\begin{pmatrix} f_1(x_1)\sqrt{w_1} & f_2(x_1)\sqrt{w_1} & \cdots & f_n(x_1)\sqrt{w_1} \\ f_1(x_2)\sqrt{w_2} & f_2(x_2)\sqrt{w_2} & \cdots & f_n(x_2)\sqrt{w_2} \\ \vdots & \vdots & \ddots & \vdots \\ f_1(x_m)\sqrt{w_m} & f_2(x_m)\sqrt{w_m} & \cdots & f_n(x_m)\sqrt{w_m} \end{pmatrix}.$$

The resulting vectors give the scaled values of an orthonormal basis for the subspace S at the nodes x_j . Note that the values of the orthonormal basis functions at any point in the interval $[0, 1]$ can be computed via interpolation given their values at the nodes x_j . This basis is then used as an input to the procedure described above for computing a quadrature formula for functions in the subspace S .

2. DISCRETIZATION OF WEAKLY SINGULAR INTEGRAL OPERATORS ON SURFACES

We now describe an approach to the discretization of integral operators of the form

$$Tf(x) = \iint_{\Sigma} K(x, y) f(y) ds(y),$$

where K is a weakly singular kernel associated with an elliptic boundary value problem and Σ is a piecewise surface. Throughout we view our operators as acting on spaces of square integrable functions and discretize them as such. The principal advantage of doing so is that the integral equations of potential theory and scattering theory are generally well-conditioned when viewed as operators on spaces of square integrable functions, even when the underlying domain of definition is Lipschitz. For further discussion of this issue and the difficulties which arise from the use of standard Nyström or collocation methods see [3, 4]. More on the properties of integral operators given on Lipschitz domains can be found in [8, 7, 9, 17]. Note that the approach of this section is directly analogous to the method for the discretization of the integral operators of scattering theory on planar domains with corner points described in Section 2 of [3].

2.1. Decompositions of surfaces. For our purposes, a decomposition D of a surface $\Sigma \subset \mathbb{R}^3$, is a finite sequence

$$D = \{\rho_j : \Delta^1 \rightarrow \Sigma\}_{j=1}^m$$

of smooth mappings with non-vanishing Jacobian determinants such that the sets $\rho_j(\Delta^1)$ form a disjoint union of Σ . Here, Δ^1 once again denotes the simplex

$$\{(x, y) \in \mathbb{R}^2 : 0 \leq x \leq 1, 0 \leq y \leq 1 - x\}.$$

We will now associate with each positive integer N and decomposition D a subspace S of $L^2(\Sigma)$ and a mapping Φ of S into a complex Cartesian space. This construction is the basis of our discretization scheme.

For each $j = 1, \dots, m$, we define S_j to be the subspace of $L^2(\Sigma)$ consisting of all functions $f : \Sigma \rightarrow \mathbb{C}$ of the form

$$f(q) = \begin{cases} g(\rho_j^{-1}(q)) |d\rho_j(\rho_j^{-1}(q))^t \cdot d\rho_j(\rho_j^{-1}(q))|^{-1/2} & \text{for } q \in \rho_j(\Delta^1) \\ 0 & \text{for } q \notin \rho_j(\Delta^1) \end{cases},$$

where g is in the space \mathcal{P}_N of polynomials of degree at most N on the simplex and $d\rho(q)$ denotes the Jacobian matrix of the parameterization ρ at the point q . Clearly, S_j is isomorphic to the Hilbert space \mathcal{P}_N of polynomials of degree N on Δ^1 endowed with the usual inner product, which is of dimension $l = (N+1)(N+2)/2$. Let $\Phi_j : S_j \rightarrow \mathbb{C}^l$ denote the mapping defined by

$$\Phi_j(f) = \begin{pmatrix} f(\rho_j(x_1, y_1)) \sqrt{w_1} |d\rho_j(x_1, y_1)^t \cdot d\rho_j(x_1, y_1)|^{1/2} \\ f(\rho_j(x_2, y_2)) \sqrt{w_2} |d\rho_j(x_2, y_2)^t \cdot d\rho_j(x_2, y_2)|^{1/2} \\ \vdots \\ f(\rho_j(x_l, y_l)) \sqrt{w_l} |d\rho_j(x_l, y_l)^t \cdot d\rho_j(x_l, y_l)|^{1/2} \end{pmatrix}, \quad (16)$$

where

$$(x_1, y_1), \dots, (x_l, y_l), w_1, w_2, \dots, w_l$$

are the nodes and weights of the Vioreanu-Rokhlin quadrature rule of order N . The subspace S is now defined as the union of the spaces S_j and the mapping $\Phi : S \rightarrow \mathbb{C}^{lm}$ is given by

$$\Phi(f) = \begin{pmatrix} \Phi_1(f_1) \\ \Phi_2(f_2) \\ \vdots \\ \Phi_m(f_m) \end{pmatrix}, \quad (17)$$

where f_j denotes the restriction of the function f to the subspace S_j .

We close this section by introducing a few pieces of terminology for mathematical objects associated with a decomposition. The sets $\rho_j(\Delta^1)$ will be known as surface elements. We shall refer to the points

$$\rho_j(x_i, y_i), \quad j = 1, \dots, m, \quad i = 1, \dots, l,$$

as the discretization nodes of the decomposition and the points

$$\rho_j(x_i, y_i), \quad i = 1, \dots, l,$$

as the discretization nodes of the surface element $\rho_j(\Delta^1)$. And, given a function f on Σ which is defined at these discretization nodes, we shall call the unique function g in the subspace S such that

$$f(\rho_j(x_i, y_i)) = g(\rho_j(x_i, y_i)), \quad j = 1, \dots, m, \quad i = 1, \dots, l,$$

the interpolant of f in S .

2.2. Discretization of integral operators acting on spaces of square integrable functions. A decomposition

$$D = \{\rho_j : \Delta^1 \rightarrow \Sigma\}_{j=1}^m$$

of a surface Σ gives rise to a scheme for the discretization of certain operators acting on the space $L^2(\Sigma)$ of square integrable functions on Σ . Let N be a positive integer and denote by $S \subset L^2(\Sigma)$ and $\Phi : S \rightarrow \mathbb{C}^{ml}$ the subspace and mapping associated with the decomposition D and integer N , as defined in the preceding section. Note that $l = (N+1)(N+2)/2$. Also, designate by P the mapping which takes functions f on Σ which are defined at the discretization nodes of the decomposition D to the interpolant of f in the subspace S .

If $T : L^2(\Gamma) \rightarrow L^2(\Gamma)$ is such that Tf is defined at each of the discretization nodes of D whenever f is a function in S , then we call the $ml \times ml$ matrix A such that the diagram

$$\begin{array}{ccc} S \subset L^2(\Gamma) & \xrightarrow{PT} & S \subset L^2(\Gamma) \\ \downarrow \Phi & & \downarrow \Phi \\ \mathbb{C}^{ml} & \xrightarrow{A} & \mathbb{C}^{ml} \end{array} \quad (18)$$

commutes the discretization of the operator T induced by the decomposition D .

2.3. Numerical approximation of the matrices discretizing weakly singular boundary integral operators arising from elliptic boundary value problems. We now describe a method for the numerical approximation of the entries of the matrix A defined by the diagram (18) in the event that T is a weakly singular boundary integral operator of the form

$$Tf(q) = \iint_{\Sigma} K(q,p)f(p)ds(p)$$

arising from an elliptic partial differential operator. Let

$$(x_{1,j}, y_{1,j}), \dots, (x_{l,j}, y_{l,j}), w_{1,j}, \dots, w_{l,j}$$

denote the nodes and weights of the discretization nodes associated with the j^{th} parameterization

$$\rho_j : \Delta^1 \rightarrow \Sigma$$

of the decomposition D . In order to describe the construction of the matrix A , we first decompose it as

$$A = \begin{pmatrix} A_1 & A_2 & \dots & A_m \end{pmatrix}$$

with each A_j a $ml \times l$ matrix. Obviously, the submatrix A_j is the mapping which takes scaled values

$$f(x_{i,j}, y_{i,j})\sqrt{w_{i,j}}, \quad i = 1, \dots, l,$$

of the function f at the discretization nodes on the surface element $\rho_j(\Delta^1)$ to the scaled values

$$\sqrt{w_{i,k}} \iint_{\Delta^1} K(\rho_k(x_{i,k}, y_{i,k}), \rho_j(x, y)) f(\rho_j(x, y)) |d\rho_j(x, y)^t \cdot d\rho_j(x, y)|^{1/2} dx dy, \quad i = 1, \dots, l, \quad k = 1, \dots, m,$$

of Tf at the discretization nodes on the entire surface Σ . In other words, each row of A_j specifies a quadrature scheme for the evaluation of an integral over the surface element $\rho_j(\Delta^1)$. The quadrature scheme used to approximate these integrals depends on the location of the ‘‘target node’’ $\rho_k(x_{i,k}, y_{i,k})$ vis-à-vis the surface element $\rho_j(\Delta^1)$.

In the event that $\rho_k(x_{i,k}, y_{i,k})$ is sufficiently distant from $\rho_j(\Delta^1)$ the relevant integral can be approximated using the quadrature associated with the discretization nodes on $\rho_j(\Delta^1)$; that is, as

$$\begin{aligned} & \iint_{\Delta^1} \sqrt{w_{i,k}} K(\rho_k(x_{i,k}, y_{i,k}), \rho_j(x, y)) f(\rho_j(x, y)) |d\rho_j(x, y)^t \cdot d\rho_j(x, y)|^{1/2} dx dy \approx \\ & \sum_{r=1}^l \sqrt{w_{i,k}} K(\rho_k(x_{i,k}, y_{i,k}), \rho_j(x_{r,j}, y_{r,j})) f(\rho_j(x_{r,j}, y_{r,j})) |d\rho_j(x_{r,j}, y_{r,j})^t \cdot d\rho_j(x_{r,j}, y_{r,j})|^{1/2} w_{r,j}. \end{aligned} \quad (19)$$

Thus we can simply take the row of the matrix A_j corresponding to the the target node to be the transpose of the vector

$$\begin{pmatrix} \sqrt{w_{i,k}} \sqrt{w_{1,j}} K(\rho_k(x_{i,k}, y_{i,k}), \rho_j(x_{1,j}, y_{1,j})) |d\rho_j(x_{1,j}, y_{1,j})^t \cdot d\rho_j(x_{1,j}, y_{1,j})|^{1/2} \\ \sqrt{w_{i,k}} \sqrt{w_{2,j}} K(\rho_k(x_{i,k}, y_{i,k}), \rho_j(x_{2,j}, y_{2,j})) |d\rho_j(x_{2,j}, y_{2,j})^t \cdot d\rho_j(x_{2,j}, y_{2,j})|^{1/2} \\ \vdots \\ \sqrt{w_{i,k}} \sqrt{w_{l,j}} K(\rho_k(x_{i,k}, y_{i,k}), \rho_j(x_{l,j}, y_{l,j})) |d\rho_j(x_{l,j}, y_{l,j})^t \cdot d\rho_j(x_{l,j}, y_{l,j})|^{1/2} \end{pmatrix}.$$

That ‘‘far interactions’’ can be handled in this fashion is the principal advantage enjoyed by Nyström methods. In the numerical experiments of this paper, a bounding sphere B_j is found for each surface element $\rho_j(\Delta^1)$ and a target point $\rho_k(x_{i,k}, y_{i,k})$ is considered to be sufficiently distant from $\rho_j(\Delta^1)$ if it is in the exterior of $2B_j$.

We say that the target node is ‘‘near’’ the surface element $\rho_j(\Delta^1)$ if it is in the interior of the sphere $2B_j$ but outside of $\rho_j(\Delta^1)$. If this is the case and the kernel K is singular, the formula (19) may not achieve sufficient accuracy. In order to construct the row of A_j corresponding to a target point $\rho_k(x_{i,k}, y_{i,k})$ in this near regime, we construct a quadrature rule with nodes and weights

$$(u_1, v_1), \dots, (u_n, v_n), \sigma_1, \dots, \sigma_n \quad (20)$$

such that

$$\begin{aligned} & \iint_{\Delta^1} \sqrt{w_{i,k}} K(\rho_k(x_{i,k}, y_{i,k}), \rho_j(x, y)) f(\rho_j(x, y)) |d\rho_j(x, y)^t \cdot d\rho_j(x, y)|^{1/2} dx dy \\ & \approx \sum_{r=1}^n \sqrt{w_{i,k}} K(\rho_k(x_{i,k}, y_{i,k}), \rho_j(u_r, v_r)) f(\rho_j(u_r, v_r)) \left| d\rho_j(u_r, v_r)^t \cdot d\rho_j(u_r, v_r) \right|^{1/2} \sigma_r \end{aligned} \quad (21)$$

whenever f is a polynomial of order N on the simplex. This is accomplished by recursively subdividing Δ^1 into triangles T_1, \dots, T_M until the target node $\rho_k(x_{i,k}, y_{i,k})$ is distant from each of the sets $\rho_j(T_s)$. Distant here means outside of $2B$, where B is a bounding ball containing the surface element $\rho_j(T_s)$. Figure 1 depicts the subdivision of the triangle Δ^1 ; subtriangles of Δ^1 are decomposed in a like manner. The nodes of the Vioreanu-Rokhlin quadrature of order N are then mapped from the simplex to each subtriangle in order to form the quadrature rule (20). Next, we form the vector

$$v = \begin{pmatrix} \sqrt{w_{i,k}} \sqrt{\sigma_1} K(\rho_k(x_{i,k}, y_{i,k}), \rho_j(u_1, v_1)) |d\rho_j(u_1, v_1)^t \cdot d\rho_j(u_1, v_1)|^{1/2} \\ \sqrt{w_{i,k}} \sqrt{\sigma_2} K(\rho_k(x_{i,k}, y_{i,k}), \rho_j(u_2, v_2)) |d\rho_j(u_1, v_1)^t \cdot d\rho_j(u_2, v_2)|^{1/2} \\ \vdots \\ \sqrt{w_{i,k}} \sqrt{\sigma_n} K(\rho_k(x_{i,k}, y_{i,k}), \rho_j(u_n, v_n)) |d\rho_j(u_n, v_n)^t \cdot d\rho_j(u_n, v_n)|^{1/2} \end{pmatrix}$$

and apply its transpose v^t on the right of the $n \times l$ interpolation matrix A which takes the scaled values

$$\begin{pmatrix} f(x_{1,j}, y_{1,j}) \sqrt{w_{1,j}} \\ f(x_{2,j}, y_{2,j}) \sqrt{w_{2,j}} \\ \vdots \\ f(x_{l,j}, y_{l,j}) \sqrt{w_{l,j}} \end{pmatrix}$$

of a polynomial of degree N on the simplex Δ^1 to its scaled values

$$\begin{pmatrix} f(u_1, v_1) \sqrt{\sigma_1} \\ f(u_2, v_2) \sqrt{\sigma_2} \\ \vdots \\ f(u_n, v_n) \sqrt{\sigma_n} \end{pmatrix}$$

at the nodes of the adaptive quadrature for the integral (21). That is, the row of the matrix A_j corresponding to the target node is the product $v^t \cdot A$, which is a vector of length l . Note that the interpolation matrix A has special structure which obviates the need to form it explicitly and allows for its rapid application. Let B denote the $4N \times N$ interpolation matrix which takes scaled values of polynomials of order N on the simplex Δ_1 to their scaled values at the nodes of the Vioreanu-Rokhlin quadratures on the subtriangles T_1, T_2, T_3 and T_4 of Δ^1 depicted in Figure 1. Then the matrix A is a product of block diagonal matrices of the form

$$\begin{pmatrix} B & 0 & 0 & 0 \\ 0 & B & 0 & 0 \\ 0 & 0 & B & 0 \\ 0 & 0 & 0 & B \end{pmatrix}$$

and it can be rapidly applied by taking this into account. Indeed, if k recursive subdivisions are required to form the quadrature (20), then only $16kN^2$ operations are required to apply the $(4N)^k \times N$ interpolation matrix A .

When the target node is one of the discretization nodes $\rho_j(x_{i,j}, y_{i,j})$ on the surface element $\rho_j(\Delta^1)$, the procedure used to form the corresponding row of A_j is almost identical. The only differences are that rather than forming a quadrature rule adaptively, we make use of the procedure for the evaluation of singular integrals described in Section 3 and the interpolation matrix no longer has special structure which allows for its rapid application.

Remark 2.1. In order to simplify the discussion in this section, we have made the assumption that the entire matrix A is being formed at once. However, the procedure described here can be trivially modified so as to obtain a method for the evaluation of individual entries of the matrix A .

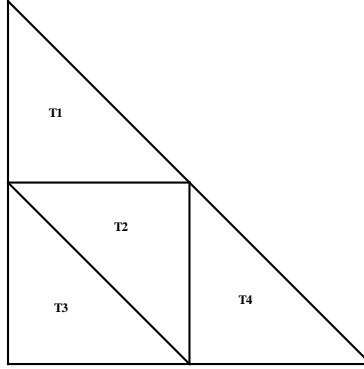


FIGURE 1. In order to evaluate near interactions, the integration domain is recursively subdivided in the manner seen here.

3. EVALUATION OF THE SINGULAR INTEGRALS ARISING FROM THE NYSTRÖM DISCRETIZATION OF WEAKLY SINGULAR INTEGRAL OPERATORS

The Nyström method described in the preceding section requires quadrature rules for the evaluation of integrals of the form

$$\iint_{\Delta^1} K(\rho(x_0, y_0), \rho(x, y)) f(\rho(x, y)) |d\rho(x, y)^t \cdot d\rho(x, y)|^{1/2} dx dy, \quad (22)$$

where K is a weakly singular kernel associated with an elliptic partial differential operators, f is a smooth function,

$$\rho : \Delta^1 \rightarrow \Sigma$$

is a smooth parameterization, (x_0, y_0) is a point in the interior of Δ^1 and $d\rho(x, y)$ denotes the Jacobian matrix of ρ at the point (x, y) . One of the standard approaches to the numerical approximation of these integrals calls for first changing the variables of integration so as to eliminate the singularity in the kernel K and then applying an adaptive integration procedure to the resulting smooth integrand [2, 10, 15].

A change to polar coordinates is one of the most commonly used mechanisms for eliminating the kernel singularity (the Duffy transform is another popular option). It is well known (see, for instance, [14]) that if K is a weakly singular kernel arising from an elliptic boundary value problem, then there exist functions f_{-1}, f_0, f_1, \dots , which are periodic and analytic on a strip containing the real line, such that

$$K(\rho(x_0, y_0), \rho(x_0 + r \cos(\theta), y_0 + r \sin(\theta))) = \frac{f_{-1}(\theta)}{r} + f_0(\theta) + f_1(\theta)r + f_2(\theta)r^2 + \dots \quad (23)$$

for all $\theta \in [0, 2\pi]$ and all $r > 0$ such that $(x_0 + r \cos(\theta), y_0 + r \sin(\theta)) \in \Delta^1$. By introducing an auxiliary parameterization

$$\xi(x, y) = \rho \left(\Phi \begin{pmatrix} x \\ y \end{pmatrix} + \Phi \begin{pmatrix} x_0 \\ y_0 \end{pmatrix} \right)$$

with Φ an appropriately chosen rotation matrix, we can rewrite the integral (22) as

$$\iint_T K(\xi(0, 0), \xi(x, y)) f(\xi(x, y)) |d\xi(x, y)^t \cdot d\xi(x, y)|^{1/2} dx dy,$$

where T is a triangle one of whose vertices is $(1, 0)$. After changing to polar coordinates, this integral takes on the form

$$\int_0^{2\pi} \int_0^{R(\theta)} K(\xi(0, 0), \xi(r \cos(\theta), r \sin(\theta))) f(\xi(r \cos(\theta), r \sin(\theta))) |d\xi(r \cos(\theta), r \sin(\theta))^t \cdot d\xi(r \cos(\theta), r \sin(\theta))|^{1/2} r dr d\theta.$$

Here, $R(\theta)$ gives a parameterization of the boundary of T in polar coordinates. We now subdivide the integration domain of the outer integral as

$$\begin{aligned}
 & \int_0^{\theta_1} \int_0^{R(\theta)} K(\xi(0, 0), \xi(r \cos(\theta), r \sin(\theta))) f(\xi(r \cos(\theta), r \sin(\theta))) \\
 & \quad |d\xi(r \cos(\theta), r \sin(\theta))^t \cdot d\xi(r \cos(\theta), r \sin(\theta))|^{1/2} r dr d\theta \\
 & + \int_{\theta_1}^{\theta_2} \int_0^{R(\theta)} K(\xi(0, 0), \xi(r \cos(\theta), r \sin(\theta))) f(\xi(r \cos(\theta), r \sin(\theta))) \\
 & \quad |d\xi(r \cos(\theta), r \sin(\theta))^t \cdot d\xi(r \cos(\theta), r \sin(\theta))|^{1/2} r dr d\theta \\
 & + \int_{\theta_2}^{2\pi} \int_0^{R(\theta)} K(\xi(0, 0), \xi(r \cos(\theta), r \sin(\theta))) f(\xi(r \cos(\theta), r \sin(\theta))) \\
 & \quad |d\xi(r \cos(\theta), r \sin(\theta))^t \cdot d\xi(r \cos(\theta), r \sin(\theta))|^{1/2} r dr d\theta,
 \end{aligned} \tag{24}$$

where θ_1 and θ_2 are such that $R(\theta)$ is smooth on the intervals $(0, \theta_1)$, (θ_1, θ_2) and $(\theta_2, 2\pi)$. It can be readily verified that while the functions obtained by restricting $R(\theta)$ to the intervals $(0, \theta_1)$, (θ_1, θ_2) and $(\theta_2, 2\pi)$ have poles on the real axis, they are nevertheless analytic in a neighborhood of their respective domains of integration. By (23), the integrands in (24) are entire as functions of r and they are analytic on a strip containing the real axis when viewed as functions of θ . It follows that applying tensor products of n -point Gaussian quadrature rules to each of the integrals in (24) separately yields an exponentially converging sequence of approximations of the definite integral (22).

Although it is tempting to conclude that exponential convergence is sufficient to guarantee that a numerical scheme is computationally viable, in this case it is simply not so. The poles of the coefficients $f_j(\theta)$ in (23) and those of the functions obtained by restricting $R(\theta)$ can severely retard the convergence of approximations of the outer integrals in (24) formed using Gaussian quadrature. If

$$H(z) = \sum_{n=0}^{\infty} a_n P_n(z) \tag{25}$$

is an expansion of a function $H(z)$ in terms of Jacobi polynomials and S is the sum of the semi-axes of the largest ellipse with foci ± 1 on which $H(z)$ is analytic, then we have

$$\liminf_{n \rightarrow \infty} |a_n|^{-1/n} = S$$

and the error in approximations of the value of the integral

$$\int_{-1}^1 H(z) dz$$

obtained via n -point Gaussian rules is expected to behave roughly as

$$O(e^{-n \log S}).$$

A statement of this result can be found, for instance, in Chapter 9 of [18].

If we write the Jacobian matrix $d\rho(x_0, y_0)$ of the parameterization ρ at the point (x_0, y_0) as

$$d\rho(x_0, y_0) = \begin{pmatrix} a_1 & b_1 \\ a_2 & b_2 \\ a_3 & b_3 \end{pmatrix},$$

then it can be shown through elementary means that each of the coefficients $f_j(\theta)$ in (23) is of the form

$$\frac{f(\theta)}{\sqrt{a \sin^2(\theta) + b \cos^2(\theta) + c \sin(2\theta)}}, \tag{26}$$

where f is a trigonometric polynomials of finite order and

$$\begin{aligned} a &= a_1^2 + a_2^2 + a_3^2 \\ b &= b_1^2 + b_2^2 + b_3^2 \\ c &= a_1 b_1 + a_2 b_2 + a_3 b_3. \end{aligned}$$

The rate of convergence of approximations of each of the integrals in (24) obtained via Gaussian quadrature is controlled by the domain of analyticity of the function

$$g(\theta) = \frac{1}{\sqrt{a \sin^2(\theta) + b \cos^2(\theta) + c \sin(2\theta)}}$$

and by the domain of analyticity of the associated restriction of $R(\theta)$. Clearly, it can happen that the poles of the function $g(\theta)$ lie close to the real axis. This occurs, for instance, when the eigenvalues of the Jacobian $d\rho(x_0, y_0)$ differ greatly in magnitude. Similarly, when the triangle T has large aspect ratio or its boundary is close to the origin, the restrictions of $R(\theta)$ become nearly singular. In some cases, the adaptive evaluation of integrals of the form (22) becomes prohibitively expensive as a result (see, for instance, the experiments of Section 4.2).

In what follows, we describe a method for the approximation of singular integrals of the form (22). It operates by first modifying the parameterization ρ in order to ensure that the linearization $d\rho(x_0, y_0)$ of ρ at (x_0, y_0) is conformal. When this is the case, the function $g(\theta)$ is a constant and the $f_j(\theta)$ are trigonometric polynomials of finite order. Then, a table of precomputed quadrature rules is applied to the outer integrals in (24) and a Legendre rule of the appropriate order is applied to the inner integrals. The size of resulting quadrature formula is not strongly dependent on the behavior of the function $R(\theta)$. This allows for the efficient evaluation of the singular integrals (22) in many cases where adaptive integration performs poorly.

Remark 3.1. Here, we have used the polar coordinate transform to illustrate the difficulties involved in the evaluation of the integrals (22). Similar difficulties are encountered when other mechanisms (such as the Duffy transform and hp adaptive methods) are used to evaluate the singular integrals arising in the discretization of weakly singular operators

3.1. Simplification of the integrand. In order to evaluate a singular integral of the form

$$\iint_{\Delta^1} K(\rho(x_0, y_0), \rho(x, y)) f(\rho(x, y)) |d\rho(x, y)^t \cdot d\rho(x, y)|^{1/2} dx dy,$$

with $(x_0, y_0) \in \Delta^1$, we first compose the user-supplied parameterization ρ with an invertible affine mapping $A: \mathbb{R}^2 \rightarrow \mathbb{R}^2$ such that $A(0, 0) = (x_0, y_0)$ and the Jacobian of the composed mapping $\tilde{\rho} = \rho \circ A$ is orthogonal at the point $(0, 0)$. Such a mapping can be constructed by computing a singular value decomposition

$$d\rho(x_0, y_0) = U \Sigma V^*$$

and taking A to be

$$A(x, y) = V \Sigma^{-1} \begin{pmatrix} x \\ y \end{pmatrix} + \begin{pmatrix} x_0 \\ y_0 \end{pmatrix}.$$

It follows, of course, that the Jacobian of the composed mapping $\tilde{\rho}$ is conformal at $(0, 0)$. In accordance with (26), the coefficients $f_j(\theta)$ in the expansion

$$K(\tilde{\rho}(0, 0), \tilde{\rho}(r \cos(\theta), r \sin(\theta))) = \frac{f_{-1}(\theta)}{r} + f_0(\theta) + f_1(\theta)r + f_2(\theta)r^2 + \dots \quad (27)$$

are trigonometric polynomials of finite order. Changing the variables of integration in

$$\iint_{A^{-1}(\Delta^1)} K(\tilde{\rho}(0, 0), \tilde{\rho}(x, y)) f(\tilde{\rho}(x, y)) |d\tilde{\rho}(x, y)^t \cdot d\tilde{\rho}(x, y)|^{1/2} dx dy. \quad (28)$$

to polar coordinates centered at the origin yields the integral

$$\begin{aligned} \int_0^{2\pi} \int_0^{R(\theta)} K(\tilde{\rho}(0, 0), \tilde{\rho}(r \cos(\theta), r \sin(\theta))) f(\tilde{\rho}(r \cos(\theta), r \sin(\theta))) \\ |d\rho(r \cos(\theta), r \sin(\theta))^t \cdot d\rho(r \cos(\theta), r \sin(\theta))|^{1/2} r dr d\theta, \end{aligned} \quad (29)$$

where $R(\theta)$ is a parameterization of the boundary of the triangle $T = A^{-1}(\Delta^1)$ in polar coordinates. By itself, this mechanism is not usually effective. While the integrand in (29) is now much more amenable to approximation via tensor products of polynomials, in most cases the introduction of the mapping A makes the approximation of the function $R(\theta)$ parameterizing the boundary of the domain of integration via polynomials more difficult.

In order to overcome this difficulty, we use a collection of precomputed quadrature rules to evaluate the integral (29) efficiently. In cases where the function $R(\theta)$ appearing in (29) is nearly singular, this approach is substantially more efficient than the usual adaptive integration methods.

3.2. Quadrature rules for a class of singular integrals. Here, we describe a method for the evaluation of singular integrals of the form (28) which depends on a table of numerically constructed quadrature formulae. We proceed by first dividing the triangle $A^{-1}(\Delta^1)$ into three subtriangles T_1 , T_2 , and T_3 by connecting the origin to each of its vertices. The integral (28) is evaluated as

$$\begin{aligned} & \iint_{T_1} K(\tilde{\rho}(0, 0), \tilde{\rho}(x, y)) f(\tilde{\rho}(x, y)) |d\tilde{\rho}(x, y)^t \cdot d\tilde{\rho}(x, y)|^{1/2} dx dy \\ & + \iint_{T_2} K(\tilde{\rho}(0, 0), \tilde{\rho}(x, y)) f(\tilde{\rho}(x, y)) |d\tilde{\rho}(x, y)^t \cdot d\tilde{\rho}(x, y)|^{1/2} dx dy \\ & + \iint_{T_3} K(\tilde{\rho}(0, 0), \tilde{\rho}(x, y)) f(\tilde{\rho}(x, y)) |d\tilde{\rho}(x, y)^t \cdot d\tilde{\rho}(x, y)|^{1/2} dx dy; \end{aligned}$$

that is, the integral is computed over each of the subtriangles separately. By applying rotations and scalings, which do not affect the representation (27), we can assume that each T_j is a triangle with vertices

$$(0, 0), (1, 0), (r_0 \cos(\theta_0), r_0 \sin(\theta_0)), \quad (30)$$

where $0 < \theta_0 < \pi$ and $0 < r_0 < 1$. If we define

$$\gamma_{r_0, \theta_0}(u) = \frac{r_0 \sin(\theta_0)}{r_0 \sin(\theta_0 - \theta_0 u) + \sin(\theta_0 u)},$$

then the integral

$$\iint_T K(\tilde{\rho}(0, 0), \tilde{\rho}(x, y)) f(\tilde{\rho}(x, y)) |d\tilde{\rho}(x, y)^t \cdot d\tilde{\rho}(x, y)|^{1/2} dx dy$$

over the triangle T with vertices (30) can be written as

$$\int_0^1 \int_0^{\gamma_{r_0, \theta_0}(u)} (f_{-1}(\theta_0 u) + f_0(\theta_0 u)r + f_1(\theta_0 u)r^2 + \dots) g(r, \theta_0 u) \theta_0 dr du \quad (31)$$

with the f_j as in (27) and g a function entire in the variables r and θ .

Our approach allows for the evaluation of integrals of the form

$$\int_0^1 \int_0^{\gamma_{r_0, \theta_0}(u)} (f_{-1}(\theta_0 u) + f_0(\theta_0 u)r + f_1(\theta_0 u)r^2 + \dots + f_n(\theta_0 u)r^{n+1}) \theta_0 dr du,$$

where f_i is a trigonometric polynomial of order $3(i+1) + 2$. The inner integral in (3.2) can be evaluated using the Legendre quadrature rule of length $\lceil n/2 \rceil + 1$ on the interval $[0, \gamma_{r_0, \theta_0}(u)]$. It is the outer integral, which can be rewritten as

$$\int_0^1 \left(f_{-1}(\theta_0 u) \gamma_{r_0, \theta_0}(u) + f_0(\theta_0 u) \frac{\gamma_{r_0, \theta_0}^2(u)}{2} + f_1(\theta_0 u) \frac{\gamma_{r_0, \theta_0}^3(u)}{3} + \dots + f_n(\theta_0 u) \frac{\gamma_{r_0, \theta_0}^{n+2}(u)}{n+2} \right) \theta_0 du,$$

that our specialized quadrature rules are designed to approximate.

Truncating the expansion in (31) has a number of implications. First, the limitation on the order of the trigonometric polynomials f_j means that our quadrature rules will only be effective for a restricted class of weakly singular kernels. The orders $3(i+1) + 2$ for the trigonometric polynomials were chosen so that the quadratures are effective for operators whose kernels are Green's functions of linear elliptic operators or first derivatives of Green's functions of linear elliptic operators. Second, as a result of using expansions which are of bounded order in the variable r , we will incur an error which depends algebraically on the diameter of the triangle T . This is contrast to adaptive integration methods which obtain a prescribed accuracy regardless of the integration domain. The rate of convergence of our Nyström scheme *in toto* will not generally be affected,

however. Assuming that sufficiently high order is chosen for the singular quadratures, the overall error in the scheme is dominated by the error arising from polynomial approximation of solutions of the integral equations.

Each quadrature rule holds for a range of values of r_0 and θ_0 and for a set value of the integer n . We refer to n as the order of the quadrature rule. We computed tables of quadrature formulae of orders 4, 8 and 16. Each table includes 88 quadrature rules which apply to values of r_0 as small as 1.0×10^{-7} and as large as 1 and for values of θ_0 as small as 1.0×10^{-7} and as large as 3.14159. The quadrature rule of order n which holds for values of r_0 and θ_0 such that

$$\alpha_{\min} < r_0 < \alpha_{\max} \text{ and } \beta_{\min} < \theta_0 < \beta_{\max}$$

is constructed by letting

$$\alpha_1, \dots, \alpha_{16} \text{ and } \beta_1, \dots, \beta_{16}$$

be the nodes of the 16-point Legendre quadratures on the intervals $[\alpha_{\min}, \alpha_{\max}]$ and $[\beta_{\min}, \beta_{\max}]$, respectively, and applying the algorithm of Section 1.3 to the functions

$$\beta_l \frac{\gamma_{\alpha_k, \beta_l}^{i+2}(u)}{i+2} \cos(j\beta_l u) \quad \text{and} \quad \beta_l \frac{\gamma_{\alpha_k, \beta_l}^{i+2}(u)}{i+2} \sin(j\beta_l u),$$

where i, j, k and l are allowed to vary as

$$i = -1, \dots, n, \quad j = 0, \dots, 3(i+1) + 2, \quad k = 1, \dots, 16, \quad l = 1, \dots, 16.$$

In order to achieve high accuracy, we performed these computations using extended precision arithmetic and requested accuracy of 1.0×10^{-16} . If the computations are instead performed using double precision arithmetic, accuracy on the order of 1.0×10^{-12} can be achieved. The lengths of the resulting quadrature rules vary from 8 to 55. See Section 4 for a

4. NUMERICAL EXPERIMENTS

We now describe several numerical experiments conducted to measure the performance of the approach of this article. All code was written in Fortran 77 and compiled with the Intel Fortran Compiler version 12.1. The experiments were carried out on a workstation equipped with 12 Intel Xeon processor cores running at 3.47 GHz and 192 GB of RAM.

In some experiments, the performance of the precomputed quadratures of Section 3 was compared to that of an adaptive procedure for the evaluation of integrals of the form

$$\iint_T f(x, y) dx dy,$$

where T is a triangle and $f(x, y)$ is a function with a radial singularity at a point (s_0, t_0) . The procedure used is representative of the most common schemes for evaluating the singular integrals arising in boundary element methods and it proceeds as follows. First, the triangle T is divided into three subtriangles by connecting the point (s_0, t_0) to each of the vertices of T . Then, the integral over each subtriangle is evaluated by writing it in the form

$$\int_0^{\theta_0} \int_0^{R(\theta)} f(s_0 + r \cos(\theta), t_0 + r \sin(\theta)) r dr d\theta, \quad (32)$$

where $R(\theta)$ smooth on $[0, \theta_0]$, and applying the procedure described by the following pseudocode:

- (1) Set $n = 6$.
- (2) Set $m = 6$.
- (3) Let $n = n + 4$.
- (4) Let $m = m + 4$.
- (5) Approximate the integral (32) using a tensor product quadrature rule formed by applying an n -point Legendre quadrature rule to the outer integral and an m -point Legendre quadrature rule to the inner integral. Denote this value by $E_{n,m}$.
- (6) If $m = 10$, goto Step 4.
- (7) If $|E_{n,m} - E_{n,m-4}| > \epsilon |E_{n,m}|$ then goto Step 4.
- (8) Let $\tilde{E}_n = E_{n,m}$.
- (9) If $n = 10$, goto Step 3.

- (10) If $|\tilde{E}_n - \tilde{E}_{n-4}| > \epsilon |\tilde{E}_n|$ then goto Step 3.
- (11) Terminate the process and return \tilde{E}_n as the approximate value of the integral and return the product quadrature used to form the value $E_{n,m}$.

4.1. **Singular integrals on triangles.** In our first set of experiments, we numerically evaluated a number of integrals of the form

$$\iint_{T_\alpha} f(x,y) dx dy$$

with

$$T_\alpha = \{(x,y) : 0 \leq x \leq 1, 0 \leq y \leq \alpha - \alpha x\}$$

and $f(x,y)$ defined almost everywhere by the formula

$$f(r \cos(\theta), r \sin(\theta)) = \frac{\cos(2\theta)}{r}. \tag{33}$$

Each integral was evaluated in three different ways: using the adaptive quadrature procedure described at the beginning of this section with a requested accuracy of $\epsilon = 1.0 \times 10^{-12}$, with the 4th order precomputed quadratures of Section 3 and analytically. The purpose of these experiments was to compare the behavior of the precomputed quadrature formulas with a standard adaptive integration technique as the integration domain becomes increasingly stretched.

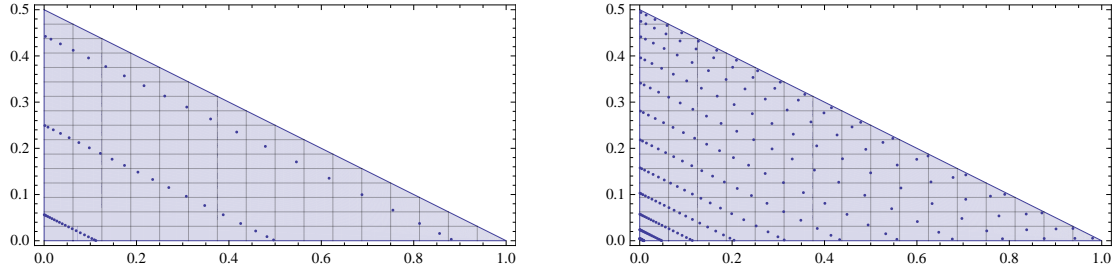


FIGURE 2. The nodes of the precomputed quadrature (left) and those of the adaptive quadrature (right) used to evaluate the integral of the function $f(x,y)$, where f is defined by (33), over the triangle $T_{1/2}$.

Table 1 presents the results. There, N_{adap} is the number of nodes required by the adaptive procedure, E_{adap} is the relative error in the approximation of the integral by adaptive quadrature, N_{precomp} is the number of nodes required to evaluate the integral using precomputed quadrature rules and E_{precomp} is the relative error in the approximation of the integral obtained via precomputed quadrature rules.

α	N_{adap}	E_{adap}	N_{precomp}	E_{precomp}
1/2	854	2.03×10^{-15}	84	2.38×10^{-16}
1×10^{-1}	1078	1.79×10^{-15}	84	1.46×10^{-15}
1×10^{-2}	1302	1.46×10^{-15}	84	8.34×10^{-16}
1×10^{-3}	1526	4.64×10^{-15}	84	3.10×10^{-16}
1×10^{-4}	1862	1.12×10^{-14}	81	5.49×10^{-16}
1×10^{-5}	2826	4.08×10^{-14}	81	3.98×10^{-16}
1×10^{-7}	11986	9.02×10^{-13}	81	3.98×10^{-16}

TABLE 1. The results of the experiments of Section 4.1.

4.2. Electrostatic layer potentials on ellipsoids. The electrostatic double layer potential generated by the unit charge distribution on a surface Σ is

$$D_0(q) = \frac{1}{4\pi} \iint_{\Sigma} \frac{(p-q) \cdot \eta_p}{|q-p|^3} ds(p),$$

where η_p denotes the outward unit normal vector to Σ at the point p . As is well known, when Σ is a closed simply-connected surface,

$$D_0(q) = \frac{1}{2} \quad \text{for all } q \in \Sigma.$$



FIGURE 3. Three views of the surface $\Sigma_{1/10}$ of Section 4.2.

In the experiments described here, this fact was used to compare the performance of adaptive quadrature with the precomputed formulas of Section 3. In each experiment, a value of α was fixed and the electrostatic double layer potential generated by the unit charge distribution on the ellipsoid Σ_α defined by

$$\left(\frac{x}{\alpha}\right)^2 + y^2 + z^2 = 1$$

was evaluated at a collection points on Σ_α . Three views of the Ellipsoid $\Sigma_{1/10}$ are shown in Figure 3. In each experiment Σ_α was parameterized by projecting it onto the boundary of the cube $[-1, 1]^3$; for instance, a portion of the surface was parameterized via the mapping defined for $-1 < s < 1$ and $-1 < t < 1$ by

$$\begin{pmatrix} s \\ t \\ 1 \end{pmatrix} \rightarrow \frac{1}{\sqrt{s^2 + t^2 + 1}} \begin{pmatrix} \alpha s \\ t \\ 1 \end{pmatrix}.$$

A decomposition of Σ_α was then formed by triangulating the faces of the cube $[-1, 1]^3$ and the associated discretization of the operator $D_0 : L^2(\Sigma_\alpha) \rightarrow L^2(\Sigma_\alpha)$ was constructed first using adaptive quadrature and then with the 12th order precomputed quadrature rules. Spaces of polynomials of order 12 were used in the discretization in both cases. The resulting discretizations were then used to approximate the value of D_0 at each of the discretization nodes on the surface Σ_α . Table 2 presents the results. There, N refers to the number of discretization nodes, N_{\max} is the length of the largest quadrature formula used to evaluate a singular integral, T_{self} is the wall clock time in seconds spent evaluating self interactions and E is the relative $L^2(\Sigma_\alpha)$ error in the approximation of D_0 .

4.3. Laplace's equation on tori. In the experiments described here, we solved the exterior Neumann problem

$$\begin{aligned} \Delta u &= 0 & \text{in } \Omega^c \\ \frac{\partial u}{\partial \nu} &= g & \text{on } \partial\Omega \end{aligned} \tag{34}$$

on a collection of tori parameterized over the square $[0, 2\pi] \times [0, 2\pi]$ by mappings of the form

$$\rho_\alpha(s, t) = \begin{pmatrix} 2 \cos(t) + \alpha \cos(s) \cos(t) \\ 2 \sin(t) + \alpha \cos(s) \sin(t) \\ \alpha \sin(s) \end{pmatrix}.$$

α	N	Adaptive			Precomputed		
		N_{\max}	T_{self}	E	N_{\max}	T_{self}	E
0.25	1092	4716	$1.05 \times 10^{+00}$	2.23×10^{-06}	658	1.19×10^{-01}	2.17×10^{-06}
	3822	4716	$2.80 \times 10^{+00}$	5.12×10^{-08}	693	4.12×10^{-01}	8.82×10^{-09}
	15288	4172	$9.70 \times 10^{+00}$	1.04×10^{-11}	693	$1.62 \times 10^{+00}$	3.67×10^{-12}
	61152	3724	$3.80 \times 10^{+01}$	4.20×10^{-13}	693	$6.44 \times 10^{+00}$	1.42×10^{-14}
0.10	1092	10052	$2.79 \times 10^{+00}$	2.02×10^{-05}	590	1.18×10^{-01}	2.02×10^{-05}
	3822	10052	$4.00 \times 10^{+00}$	5.10×10^{-06}	693	4.11×10^{-01}	5.11×10^{-06}
	15288	5348	$1.13 \times 10^{+01}$	7.54×10^{-12}	700	$1.61 \times 10^{+00}$	4.99×10^{-12}
0.05	1092	17788	$7.97 \times 10^{+00}$	3.29×10^{-04}	672	1.18×10^{-01}	3.29×10^{-04}
	3822	17788	$6.79 \times 10^{+00}$	1.37×10^{-05}	700	4.12×10^{-01}	1.38×10^{-05}
	15288	7572	$1.54 \times 10^{+01}$	3.00×10^{-09}	700	$1.64 \times 10^{+00}$	3.00×10^{-09}
	61152	7572	$5.01 \times 10^{+01}$	5.13×10^{-13}	700	$6.46 \times 10^{+00}$	2.84×10^{-13}
0.01	1092	213076	$1.19 \times 10^{+02}$	1.42×10^{-03}	672	1.17×10^{-01}	1.42×10^{-03}
	3822	141564	$5.80 \times 10^{+01}$	5.64×10^{-05}	693	4.83×10^{-01}	5.68×10^{-05}
	15288	118928	$8.66 \times 10^{+01}$	9.53×10^{-08}	693	$1.62 \times 10^{+00}$	9.53×10^{-08}
	61152	122548	$2.25 \times 10^{+02}$	1.80×10^{-10}	693	$6.44 \times 10^{+00}$	1.80×10^{-10}
	222768	122548	$5.08 \times 10^{+03}$	7.28×10^{-12}	693	$2.37 \times 10^{+01}$	7.28×10^{-12}

TABLE 2. The results of the experiments described in Section 4.2.

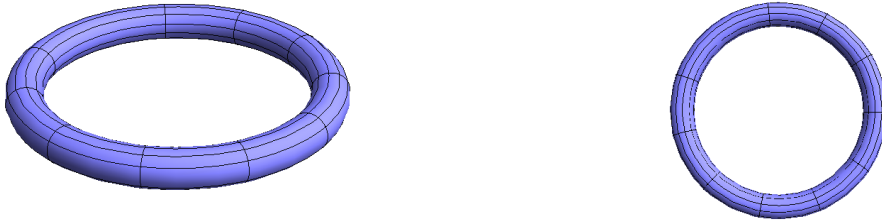
Two views of the domain parameterized by $p_{1/4}$ are shown in Figure 4. The representation

$$u(q) = \frac{1}{4\pi} \iint_{\partial\Omega} \frac{\sigma(p)}{|q-p|} ds(p)$$

of the solution u of (34) leads to the integral equation

$$\frac{1}{2}\sigma(q) + \frac{1}{4\pi} \iint_{\partial\Omega} \frac{(p-q) \cdot \eta_p}{|q-p|^3} \sigma(p) ds(p) = g(x), \quad (35)$$

which is well known to be uniquely solvable for $g \in L^2(\partial\Omega)$.


 FIGURE 4. Two views of one of the domain parameterized by the function $p_{1/4}(s, t)$, which is defined in Section 4.3.

In each experiment, the parameterization domain $[0, 2\pi] \times [0, 2\pi]$ was subdivided into triangles in order to form a decomposition of the surface. The order of the spaces of polynomials used in discretization procedure was taken to be 16 (that is, the constant N in Section 2 was set to 16) and the 16th order precomputed rules of Section 3 were used to evaluate singular integrals. The problem (34) was then solved with the boundary data taken to be the normal derivative of the potential

$$g(q) = \frac{1}{|q-p_1|} - \frac{1}{|q-p_2|},$$

where p_1 is the point $(2, 0, 0)$ and p_2 is the point $(0, 2, 0)$. A multipole code coupled with the standard GMRES algorithm was used to invert the system of linear equations which resulted from discretizing (35). The accuracy of obtained solution u was tested by computing the relative $L^2(B)$ error

$$\left(\iint_B |g(p)|^2 ds(p) \right)^{-1/2} \left(\iint_B |u(p) - g(p)|^2 ds(p) \right)^{1/2}$$

with B is the ball of radius 5 centered at the origin. Table 3 presents the results. The notation used there is as follows:

- N_{tri} specifies the number of triangles into which the parameterization domain was divided;
- N is the the total number of discretization nodes;
- N_{self} is the average number of nodes in the precomputed quadrature rules used to evaluate singular integrals;
- T_{self} is the wall clock time which was spent evaluating singular integrals;
- T_{near} is the wall clock time which was spent evaluating nearly singular integrals;
- T_{mult} is the wall clock time which was spent performing precomputations for the multipole procedure;
- T is the total wall clock time spent on the experiment;
- E is the relative error $L^2(B)$ error in the obtained solution.

The *raison d'être* for these experiments is to demonstrate that the use of the precomputed quadrature formulas does not adversely affect the rate of convergence of a boundary element method and to show that the performance of these quadrature formulae is largely independent of the behavior of parameterizations.

α	N_{tri}	N	N_{self}	T_{self}	T_{near}	T_{mult}	T_{total}	E
1.00	4	612	983	1.43×10^{-01}	$1.11 \times 10^{+00}$	2.18×10^{-01}	$1.60 \times 10^{+00}$	1.36×10^{-04}
	16	2448	978	5.83×10^{-01}	$2.84 \times 10^{+00}$	$3.44 \times 10^{+00}$	$7.86 \times 10^{+00}$	1.48×10^{-10}
	64	9792	976	$2.57 \times 10^{+00}$	$8.64 \times 10^{+00}$	$4.01 \times 10^{+01}$	$6.31 \times 10^{+01}$	8.64×10^{-14}
0.25	16	2448	976	5.60×10^{-01}	$1.63 \times 10^{+00}$	$3.23 \times 10^{+00}$	$6.31 \times 10^{+00}$	7.07×10^{-07}
	64	9792	976	$2.26 \times 10^{+00}$	$6.41 \times 10^{+00}$	$2.77 \times 10^{+01}$	$4.45 \times 10^{+01}$	2.19×10^{-11}
	256	39168	976	$8.88 \times 10^{+00}$	$2.54 \times 10^{+01}$	$1.38 \times 10^{+02}$	$2.19 \times 10^{+02}$	2.85×10^{-14}
0.10	40	6120	976	$1.42 \times 10^{+00}$	$3.34 \times 10^{+00}$	$1.09 \times 10^{+01}$	$1.92 \times 10^{+01}$	5.88×10^{-07}
	160	24480	975	$5.57 \times 10^{+00}$	$1.45 \times 10^{+01}$	$7.70 \times 10^{+01}$	$1.16 \times 10^{+02}$	1.11×10^{-11}
	640	97920	976	$2.23 \times 10^{+01}$	$5.91 \times 10^{+01}$	$5.00 \times 10^{+02}$	$6.92 \times 10^{+02}$	2.30×10^{-14}
0.01	400	61200	975	$1.38 \times 10^{+01}$	$2.86 \times 10^{+01}$	$1.05 \times 10^{+02}$	$1.79 \times 10^{+02}$	5.12×10^{-07}
	1600	244800	975	$5.54 \times 10^{+01}$	$1.32 \times 10^{+02}$	$8.47 \times 10^{+02}$	$1.20 \times 10^{+03}$	8.39×10^{-12}
	6400	979200	975	$2.22 \times 10^{+02}$	$5.94 \times 10^{+02}$	$4.76 \times 10^{+03}$	$6.70 \times 10^{+03}$	7.07×10^{-13}

TABLE 3. The results of the experiments described in Section 4.3.

4.4. An electromagnetic scattering problem. The boundary value problem

$$\begin{aligned}
\nabla \times \mathbf{E} &= ik\mathbf{H} & \text{in } \Omega^c \\
\nabla \times \mathbf{H} &= -ik\mathbf{E} & \text{in } \Omega^c \\
\nabla \cdot \mathbf{E} &= 0 & \text{in } \Omega^c \\
\nabla \cdot \mathbf{H} &= 0 & \text{in } \Omega^c \\
\eta \times \mathbf{E} &= 0 & \text{on } \partial\Omega
\end{aligned} \tag{36}$$

arises from the scattering of time-harmonic waves from a perfect conductor Ω . Here, η is the outward-pointing unit normal vector to $\partial\Omega$ and \mathbf{E} and \mathbf{H} represent the total electric and magnetic fields. That is,

$$\begin{aligned}
\mathbf{E} &= \mathbf{E}_{\text{in}} + \mathbf{E}_{\text{scat}} \\
\mathbf{H} &= \mathbf{H}_{\text{in}} + \mathbf{H}_{\text{scat}},
\end{aligned}$$

where \mathbf{E}_{in} and \mathbf{H}_{in} are incident fields and \mathbf{E}_{scat} and \mathbf{H}_{scat} denote scattered fields of interest. The magnetic field integral equation is obtained by inserting the representation

$$\mathbf{H}_{\text{scat}} = \nabla \times \mathbf{A}, \tag{37}$$

where

$$\mathbf{A}(q) = \frac{1}{4\pi} \iint_{\partial\Omega} \frac{e^{ik|q-p|}}{|q-p|} \mathbf{J}(p) ds(p),$$

into (36). Specifically, a solution to (36) of the form (37) can be obtained by solving the integral equation

$$\frac{1}{2} \mathbf{J} + \eta \times \mathbf{H}_{\text{scat}} = -\eta \times \mathbf{H}_{\text{in}}. \tag{38}$$

The unknown in (38) is the surface current \mathbf{J} given on $\partial\Omega$.

In each experiment, an instance of the boundary value problem (36) was solved by applying the discretization procedure of Section 2 to the integral equation (38) and solving the resulting linear system of equations. The 8th order quadrature rules of Section 3 were used to evaluate singular integrals and spaces of 8th order polynomials were used to represent solutions. In each case, the region Ω was taken to be the unit sphere and k was set to be 1. The incoming field \mathbf{H}_{in} was the potential generated by a unit source charge at the point $(0.2, -0.3, 0.1)$. Each obtained solution \mathbf{J} of the integral equation was used to approximate the electric field \mathbf{E} and magnetic field \mathbf{H} at the point $(10, 20, -30)$. Those values are known by the extension theorem. Table 4 presents the results. There, N_{tris} is the number of triangles into which the parameterization domain is subdivided, N is the number of discretization nodes on the surface, E_{electric} is the largest relative component-wise error in the electric field and E_{magnetic} is the largest relative component-wise error in the magnetic field.

N_{tri}	N	E_{electric}	E_{magnetic}
12	540	5.92×10^{-05}	9.25×10^{-05}
48	2160	5.46×10^{-09}	5.76×10^{-09}
192	8640	1.85×10^{-12}	3.94×10^{-12}

TABLE 4. The results of the experiments described in Section 4.4.

The principal purpose of these experiments is to show that high accuracy can be obtained using the quadratures of Section 3 and that the use of such quadratures does not retard the convergence of boundary element methods.

4.5. A singular domain. In these final experiments, we considered the exterior Neumann problem

$$\begin{aligned} \Delta u + k^2 u &= 0 && \text{in } \Omega^c \\ \frac{\partial u}{\partial \eta} &= g && \text{on } \partial\Omega \end{aligned} \tag{39}$$

$$|x| \left(\frac{\partial}{\partial |x|} - ik \right) u(x) \rightarrow 0 \text{ as } |x| \rightarrow \infty$$

in the case where Ω has singular boundary. In particular, we took Ω to be the surface parameterized over $[0, 2\pi] \times [0, \pi]$ via the mapping

$$p(s, t) = \begin{pmatrix} 2 \sin(t/2) \\ \cos(s) \sin(t) \\ \sin(s) \sin(t) \end{pmatrix}.$$

See Figure 5 for several views of this domain, which has a single corner point. By representing the solution u as

$$u(q) = \frac{1}{4\pi} \iint_{\partial\Omega} \frac{e^{ik|q-p|}}{|q-p|} \sigma(p) ds(p),$$

the boundary value problem (39) can be reformulated as the integral equation

$$-\frac{1}{2}\sigma(q) + \frac{1}{4\pi} \iint_{\partial\Omega} \frac{(q-p) \cdot \eta_p}{|q-p|^3} \exp(ik|q-p|) (1 - ik|q-p|) \sigma(p) ds(p) = g(q). \quad (40)$$

Note that for certain wavenumbers, the integral operator appearing in (40) will have a nontrivial nullspace. For the experiments of this section, the wavenumber k was taken to be 1 and this problem did not arise. Numerous approaches for addressing this difficulty have been suggested in the literature.

In each experiment, a discretization of the integral operator appearing in (40) was formed using the approach of Section 2. Spaces of 8th order polynomials were used to discretize solutions and the 8th precomputed quadrature rules of Section 3 were used to evaluate singular integrals. The condition number of each discretization was computed and each discretization was also used to solve an instance of the boundary value problem (39). The boundary data g was taken to be the normal derivative of the function

$$h(q) = \frac{e^{i|q-p_0|}}{|q-p_0|},$$

where p_0 is the point $(1, 0, 0)$. The obtained solution was compared to the true solution h of the boundary value problem (40) at the point $(10, 0, 0)$. Table 5 displays the results; there, N refers to the number of discretization nodes, κ is the condition number of the discretization and E is the relative error in the obtained solution at the point $(10, 0, 0)$.

These experiments illustrate one of the primary difference between the scheme of this paper and standard Nyström or collocation methods. Namely, that the discretizations obtained by applying the procedure of Section 2 reflect the L^2 properties of the operator. In this case, the operator in question is well-conditioned as an operator $L^2(\Sigma) \rightarrow L^2(\Sigma)$ but it is not bounded when considered as an operator on various Hölder spaces. Standard collocation and Nyström schemes, when applied to this operator, yield highly ill-conditioned discretizations while the Galerkin method and the approach of this paper result in well-conditioned matrices.

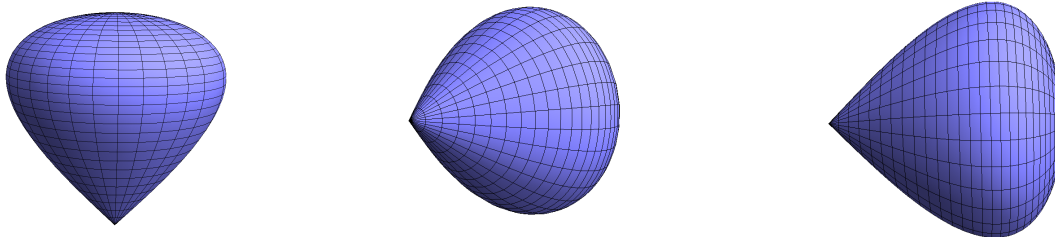


FIGURE 5. Three views of the singular domain of Section 3.

N	κ	E
180	$2.40 \times 10^{+0}$	1.52×10^{-03}
720	$2.42 \times 10^{+0}$	2.42×10^{-05}
2880	$2.44 \times 10^{+0}$	1.04×10^{-07}
11520	$2.45 \times 10^{+0}$	9.09×10^{-10}
46080	$2.45 \times 10^{+0}$	7.04×10^{-13}

TABLE 5. The results of the experiments described in Section 4.5.

5. CONCLUSIONS AND FUTURE WORK

The scheme of this paper provides a reliable and high-accuracy mechanism for discretizing integral operators with weakly singular kernels on surfaces. In the author's experience, it is a considerably more robust and efficient than schemes which utilize adaptive quadrature. It is particularly effective in cases where surface parameterizations behave poorly (i.e., are highly nonconformal).

While the performance of the scheme is good compared to existing methods, we believe that the scheme of this paper can be made still more efficient and we are pursuing several avenues of investigation:

- The procedure of Section 1.3 can be generalized to the case of collections of functions given on two-dimensional domains. It is possible to use this generalization to construct more efficient quadrature rules which are not tensor products. The computational effort required to construct such rules is considerable, however.
- Rather than compose a user-supplied parameterization ρ with an affine mapping in order to obtain a parameterization which is conformal at the target node, we could use a nonlinear transformation ϕ . This would allow for more degrees of freedom which could be exploited to, for instance, produce a mapping which takes the simplex to itself. The danger of this approach is that nonlinear mappings increase the order of the polynomials which must be integrated. It remains to be seen whether the use of nonlinear mappings in lieu of affine mappings will lead to an improved scheme.
- The authors are investigating a reparameterization scheme which, given user-specified parameterizations, constructs new parameterizations whose linearizations are conformal at the appropriate points.

6. ACKNOWLEDGEMENTS

The first author was supported by the Office of Naval Research under contract N00014-09-1-0318. The second author was supported in part by the Air Force Office of Scientific Research under NSSEFF Program Award FA9550-10-1-0180 and in part by the National Science Foundation under grant DMS-0934733.

REFERENCES

- [1] ABRAMOWITZ, M., AND STEGUN, I., Eds. *Handbook of Mathematical Functions*. Dover, New York, 1964.
- [2] ATKINSON, K. E. *The Numerical Solution of Integral Equations of the Second Kind*. Cambridge University Press, Cambridge, 1997.
- [3] BREMER, J. A fast direct solver for the integral equations of scattering theory on planar curves with corners. *Journal of Computational Physics* (to appear).
- [4] BREMER, J. On the Nyström discretization of integral operators on planar domains with corners. *Applied and Computational Harmonic Analysis* (to appear).
- [5] BREMER, J., GIMBUTAS, Z., AND ROKHLIN, V. A nonlinear optimization procedure for generalized Gaussian quadratures. *SIAM Journal of Scientific Computing* 32 (2010), 1761–1788.
- [6] CHERNOV, A., VON PETERSDORFF, T., AND SCHWAB, C. Exponential convergence of hp quadrature for integral operators with Gerver kernels. *ESAIM: Mathematical Modelling and Numerical Analysis* 45 (2011), 387–422.
- [7] COIFMAN, R. R., MCINTOSH, A., AND MEYER, Y. L'intégrale de Cauchy définit un opérateur borné sur L^2 pour les courbes Lipschitziennes. *Annals of Math* 116 (1982), 361–388.
- [8] COIFMAN, R. R., AND MEYER, Y. *Wavelets: Calderón-Zygmund and Multilinear Operators*. Cambridge University Press, Cambridge, 1997.
- [9] DAVID, G., AND JOURNÉ, J. L. A boundedness criterion for generalized Calderón-Zygmund operators. *Annals of Mathematics* 120 (1984), 371–397.
- [10] HACKBUSCH, W. *Integral Equations: theory and numerical treatment*. Birkhäuser, Berlin, 1995.
- [11] HACKBUSCH, W., AND SAUTER, S. On numerical cubatures of nearly singular surface integrals arising in BEM collocation. *Computing* 52 (1994), 139–159.
- [12] KOORNWINDER, T. Two-variable analogues of the classical orthogonal polynomials. In *Theory and Application of Special Functions*, R. Askey, Ed. 1975, pp. 435–495.
- [13] SAUTER, S., AND SCHWAB, C. Quadrature for hp -Galerkin BEM in \mathbb{R}^3 . *Numerische Mathematik* 78 (1997), 211–258.
- [14] SCHWAB, C., AND WENDLAND, W. L. Kernel properties and representation of boundary integral operators. *Mathematische Nachrichten* 156 (1992), 187–218.
- [15] SCHWAB, C., AND WENDLAND, W. L. On numerical cubatures of singular surface integrals in boundary element methods. *Numerische Mathematik* 62 (1992), 343–369.
- [16] SLADEK, V., SLADEK, J., AND TANAKA, M. Evaluation of $1/r$ integrals in BEM formulations for 3-d problems using coordinate multitransformations. *Engineering Analysis with Boundary Elements* 20 (1997), 229–244.

- [17] STEIN, E. *Harmonic Analysis*. Princeton University Press, Princeton, New Jersey, 1992.
- [18] SZEGÖ, G. *Orthogonal Polynomials*. American Mathematical Society, Providence, Rhode Island, 1959.
- [19] VIOREANU, B., AND ROKHLIN, V. Spectra of multiplication operators as a numerical tool. *Yale University Department of Computer Science Technical Report TR1443* (2011).